Energy Proceedings
Vol 26, 2022
ISSN 2004-2965

Improvement of Mathematical Model and Coefficients Identification of Adjustable Jet Pumps

Youfu Wu[1], Guang Yang [2], Hai Wang[1*]

1 School of Mechanical Engineering, Tongji University, Shanghai, China200092

*Correspondence: wanghai@tongji.edu.cn[1]

ABSTRACT

Compared with fixed jet pumps (FJPs), adjustable jet pumps (FJPs) have a wider application potential in heating and other fields. However, the existing mathematical model of FJPs cannot accurately describe the performance of AJPs. In this paper, on the basis of considering the influence of the position of the needle on the performance of the adjustable jet pump, the existing mathematical model of FJPs is improved and simplified to characterize AJPs. Furthermore, the coefficients in the mathematical model are identified by genetic algorithm. After verification, the average error between the flow rate obtained by the mathematical model and the measured value is within 2%.

Keywords: Adjustable jet pump Mathematical model Velocity coefficients identification Genetic algorithm

NONMENCLATURE

Abbreviations	
FJP	Fixed jet pump
AJP	adjustable jet pump
Symbols	
P	Pressure
G	Mass flowrate
ω	Velocity
ψ	Coefficients
f	Area
ρ	Density
m	Area ratio
u	Mixing ratio
h	Pressure ratio

1. INTRODUCTION

Jet pump is a fluid mechanical equipment that uses the lateral turbulent diffusion of high-pressure primary flow to pump low-pressure secondary flow to complete mass, energy transfer and mixing reactions. Due to high reliability and convenience of maintenance brought by simple structure and absence of moving parts, jet pumps are used widely in many fields such as water conservancy, civil engineering and transporting solids or fish(Li et al., 2019; F. Liu, Li, & Zeng, 2017; X. L. Liu, Zhan, & Lia, 2017; Long, Xu, Lyu, & Zou, 2016; Y. Lu, Liu, Wang, & Wang, 2021; Zhang et al., 2020). Jet pump can be classed into adjustable and fixed according to the area of the nozzle outlet being able to be changed or not in operation. Most of them are aimed at fixed jet pumps （FJP）, and there are relatively few studies on adjustable jet pumps(AJP) among the existing researches.

The researches on jet pumps can be summarized into three aspects: establishing mathematical model, researching performance and structural design. The mathematical model of jet pumps was established early to describe the performance of jet pumps and the reference values of the coefficients in the equations were given(H. Lu & Lu, 2011). The current research directions are performance research and structural parameter design, where experimental testing and computational fluid dynamics (CFD) are the main research methods.

Beithou et al. (Beithou & Aybar, 2000) established a mathematical model based on some simplified assumptions and compared the experimental results with the calculated values. The comparisons showed that the experimental and calculated pressure distributions were in good agreement in the mixing chamber and diffuser.

Winoto S H et al. (Winoto, Li, & Shah, 2000) studied the efficiency of the water jet pump through theoretical analysis and experimental research, derived the theoretical efficiency equation of the jet pump based on a one-dimensional formula, and designed and built a

water jet pump experimental platform for experimental research.

Iran E et al.(Neto, 2011) researched the maximum suction lift of water jet pumps with different diameters and nozzle-to-throat area ratios and concluded that the area ratio was an important parameter to characterize the maximum suction lift.

Zhu et al. (Zhu, Long, Zhang, & Lu, 2012) compared the performance difference between an adjustable jet pump and a fixed jet pump through an experimental study. The results showed that the efficiency of the former was slightly lower than the latter under close to rated conditions, and the theory of fixed jet pumps cannot be fully applied to adjustable jet pumps.

Long et al.(Long, Zhang, et al., 2016) conducted experiments on the cavitation of three jet pump cavitation reactors with three area ratios (m = 1.78, 2.56, 4.00) under varying operating conditions to achieve some guidance for the design and the choice of operating conditions for practical application of JPCR.

Aldaş et al.(Aldaş & Yapıcı, 2014) determined the effect of the scaling-up, downscaling and change in the absolute and relative roughness on the energy efficiency of the jet pumps using a CFD solver ANSYS FLUENT, and concluded that the optimum efficiencies for different area ratios over a wide range were determined according to the scale and size of roughness.

Sheha et al.(Sheha, Nasr, Hosien, & Wahba, 2018) studied the effect of diffuser angle, mixing chamber length, area ratio and driving nozzle position on the efficiency of jet pump and optimized the structural parameters by CFD.

Lívia et al.(Reis & Gioria, 2021) optimized the whole geometry of a water ejector by using CFD simulations combined with the Nelder-Mead optimization technique, and analyzed the influence of geometric parameters and different shapes of the curves on the efficiency and the resulting flow fields of the ejector.

At present, there have been many studies on jet pump performance and structural optimization design, and the mathematical model of jet pumps are no longer concerned. Because in most cases there is no need to carry out related theoretical calculations, experimental tests and simulations can meet the needs. Moreover, the flow inside jet pump is very complicated, the coefficients in the mathematical equations are unreasonable, and the calculated result has a large deviation from the actual situation. In some situations, the mathematical model of jet pump is still required for calculation, but even for adjustable jet pumps, the coefficient values in the equation are mostly the default reference values of fixed jet pumps(Wang & Wang, 2019). However, the performances of AJP and FJP are very different due to the difference in structure. Therefore, the values of the coefficients in the equations needs to be corrected.

In this study, the existing theoretical equation of FJP was improved to describe AJP. Then, an experiment on the AJP under different area ratios was carried out. Based on the experimental data, the coefficients in performance equation of the AJP under different areas are solved through genetic optimization algorithm. Finally, the relationship between each coefficient and AJP area ratio was fitted. The purpose of this paper is to propose a method to solve the coefficients in the theoretical equation of jet pump for reference by relevant scholars. At the same time, the coefficient values obtained can also be used as reference values for theoretical calculation of AJP of the same structure.

2. THE WORKING PRINCIPLE AND MATHEMATICAL MODEL OF AJP

2.1 The working principle

The structure of the AJP is shown in *Fig. 1* The general jet pump is mainly composed of four parts: nozzle, suction chamber, mixing chamber and diffuser. In order to adjust the nozzle outlet cross-sectional area to meet the demand in operation, an adjusting body—a needle is added to AJP on the basis of FJP.

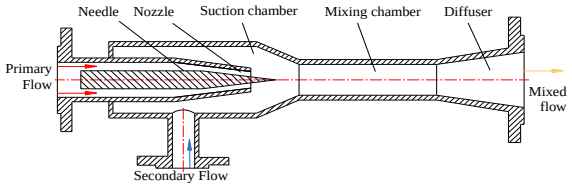

Fig. 1 The structure of the fixed jet pump

The flow in jet pump belongs to three-dimensional fluid mechanics, which is very complicated. There is no precise calculation method yet. The existing mathematical model is established on the basis of simplifying the three-dimensional flow process into one dimension and making a series of simplifications.

Fig. 2 shows a sketch of the average pressure and velocity along the longitudinal direction. The primary flow with pressure P_p and velocity w_p passes through the nozzle, the potential energy is converted into kinetic energy. On the exit cross section of the nozzle1-1, the pressure drops to P_{p1}, the velocity increases to w_{p1}, and

a specific turbulent distribution is produced. The secondary flow with pressure P_s and velocity w_s is directed into the jet pump through the suction chamber. When the two flows reach the inlet cross section of the mixing chamber 2-2, the pressure drops to P_2. Energy and mass of them are exchanged in the mixing chamber. On the exit cross section of the mixing chamber 3-3, both the pressure and the velocities of them reach the same level, which are respectively P_3 and w_3. Finally, the mixed flow passes through the diffuser tube, where the kinetic energy is converted into potential energy. When flowing out of the outlet of the diffuse, the pressure rises to P_c, and the speed drops to w_c.

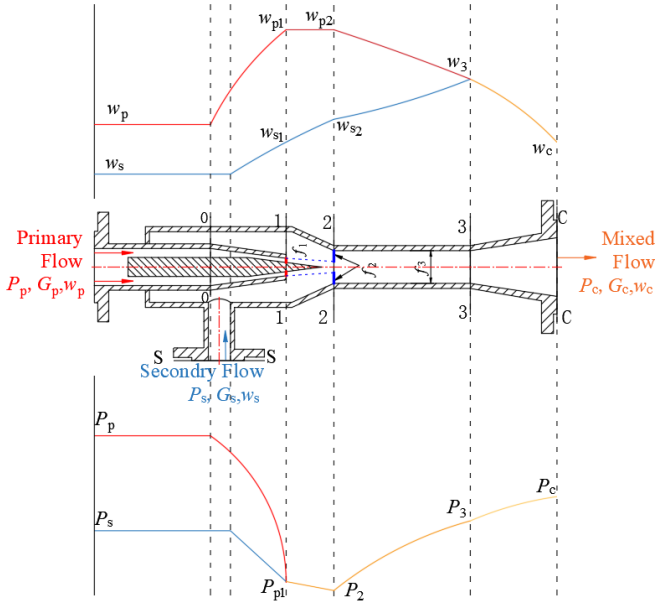

Fig. 2 A sketch of the average pressure and velocity along the longitudinal direction in jet pump

2.2 The mathematical model

The mathematical model of the jet pump is based on the conservation of mass, energy and momentum.

The mass conservation equation is written as:

$$G_c = G_p + G_s \tag{1}$$

The energy conservation equations are obtained for the nozzle, suction chamber and diffuser respectively.

The inlet velocity of the primary flow w_p is much smaller than the velocity at the nozzle w_{p1} and can be ignored. At the same time, the velocity coefficient of the nozzle φ_1 is introduced to measure the energy loss when the primary flow passes through the nozzle. The energy conservation equation of the primary fluid between the cross-sections 0-0 and 1-1 is drawn as:

$$P_p = P_s + \frac{\rho_{p1}}{2}\left(\frac{w_{p1}}{\varphi_1}\right)^2 \tag{2}$$

$$w_{p1} = \frac{G_p}{\rho_{p1} f_{p1}} \tag{3}$$

The relationship between the flow rate of the primary flow and the pressure difference between the inlets of the two flows can be obtained from the equation (2):

$$G_p = \varphi_1 f_{p1}\sqrt{2\rho_{p1}\Delta P_p} \tag{4}$$

Ignoring the velocity of the secondary flow w_s, the velocity coefficient of entrance section of mixing chamber φ_2 is introduced to measure the energy loss of the secondary flow from the suction inlet to the mixing chamber inlet. The energy conservation equation of the secondary flow between the section S-S and 2-2 is drawn as:

$$P_s = P_2 + \frac{\rho_{s2}}{2}\left(\frac{w_{s\,2}}{\varphi_2}\right)^2 \tag{5}$$

$$w_{s2} = \frac{G_s}{\rho_{s2} f_{s2}} \tag{6}$$

Similarly, the velocity coefficient of the diffuser φ_3 is introduced to measure the energy loss of the mixed flow in the diffuser, and the energy conservation equation between section 3-3 and C-C is obtained.

$$P_3 + \frac{\rho_3}{2}(\varphi_3 w_3)^2 = P_c \tag{7}$$

$$w_3 = \frac{G_c}{\rho_3 f_3} \tag{8}$$

The velocity coefficient of the mixing chamber φ_4 is used to characterize the momentum loss of the two flows in the mixing chamber due to friction, and the momentum conservation equation of them in the mixing chamber is drawn between the sections 2-2 and 3-3.

$$\varphi_4\left(G_p w_{p2} + G_s w_{s2}\right) - G_c w_3 = (P_3 - P_2) f_3 \tag{9}$$

The working medium studied in this paper is water, whose density can be considered to remain unchanged, that is, $\rho_{p1} = \rho_{p2} = \rho_{s2} = \rho_3$.

According to the above equations (1)-(8), the relationship between pressure and flow rate of the jet pump can be obtained as follows:

$$\frac{P_c - P_s}{P_p - P_s} = 2\varphi_1^2\varphi_4\frac{f_{p1}^2}{f_{p2}f_3} + 2\varphi_1^2\varphi_4\frac{f_{p1}^2}{f_{s2}f_3}\frac{G_s^2}{G_p^{\,2}} - \frac{1}{\varphi_2^2}\frac{f_{p1}^2}{f_{s2}^2}\frac{G_s^2}{G_p^{\,2}} - \varphi_1^2(2-\varphi_3^2)\frac{f_{p1}^2}{f_3^2}\frac{G_c^2}{G_p^{\,2}} \tag{10}$$

In the above equations (1) to (10), G is the mass flow, P is the pressure, w is the velocity, ρ is the density, and f is the area of the cross section. The subscripts p, s, and m respectively represent the primary flow, secondary

flow and mixed flow, the subscripts 1, 2, 3 indicate cross-sections.

Existing researches assume that the primary flow and the secondary flow are not mixed before entering the mixing chamber when establishing the above equations. The jet cross-section of the primary flow between the nozzle outlet and the inlet of the mixing chamber remains unchanged (f_{p1}=f_{p2}), but this assumption is unreasonable. The cross-section area of the primary flow sprayed from the nozzle gradually increases due to the expansion of the boundary layer. Especially when the area ratio *m* is relatively small (the nozzle outlet area is relatively large), the faster the jet cross-section of the primary flow expands. Based on this, the cross-sectional area ratio φ_5 is defined as the ratio of the cross-sectional area of the primary flow at the nozzle outlet cross-section 1-1 and the mixing chamber inlet cross-section 2-2. which is:

$$\varphi_5 = \frac{f_{p1}}{f_{p2}} \tag{11}$$

As shown in *Fig. 3*, during the movement of the needle, the top part of the needle will be in the mixing chamber. At this time, the primary flow on the inlet section of the mixing chamber is no longer a solid cylindrical jet, but a hollow annular jet. At this time, the area occupied by the secondary flow is determined by the following formula:

$$f_{s2} = f_3 - f_{p2} - f_N \tag{12}$$

Where, f_N is the cross-sectional area of the needle on the entrance section of the mixing chamber, which is determined by the distance L_c from the nozzle to the mixing chamber and the stroke of the needle *x*.

$$f_N = \pi\left[\left(\frac{d_1}{\tan\frac{\alpha}{2}} - L_c - x\right)\tan\frac{\alpha}{2}\right]^2 \tag{13}$$

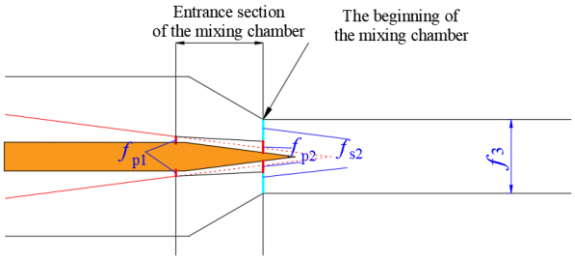

Fig. 3 The position where the top of the needle is in the mixing chamber during the movement

At present, the dimensionless parameters pressure ratio *h*, flow ratio *u* and area ratio *m* are commonly used to characterize the performance of jet pumps. They are defined as follows:

$$h = \frac{\Delta P_c}{\Delta P_p} = \frac{P_c - P_s}{P_p - P_s} \tag{14}$$

$$u = \frac{G_s}{G_p} \tag{15}$$

$$m = \frac{f_3}{f_1} \tag{16}$$

On the basis of the above equations, the following characteristic equation of AJP can be derived, which shows the relationship between the pressure ratio *h*, the area ratio *m* and the flow ratio *u*.

$$h = \frac{2\varphi_1^2\varphi_4\varphi_5}{m} + 2\varphi_1^2\varphi_4\varphi_5\frac{u^2}{m(\varphi_5 m - 1 - m_N)} - \frac{\varphi_1^2\varphi_5^2}{\varphi_2^2}\frac{u^2}{(\varphi_5 m - 1 - m_N)^2} - \varphi_1^2(2-\varphi_3^2)\frac{(1+u)^2}{m^2} \tag{17}$$

where, $m_N = f_N/f_{p1}$.

When using the above equation to calculate the adjustable jet pump, it is necessary to determine the positional relationship between the top of the jet needle and the inlet of the mixing chamber in advance to calculate m_N. In order to eliminate the m_N in the equation (17), only the pressure difference ratio *h*, the mixing ratio *u* and the area ratio *m* are used to describe the characteristics of the AJP. This paper makes the following simplifications shown in *Fig. 4*.

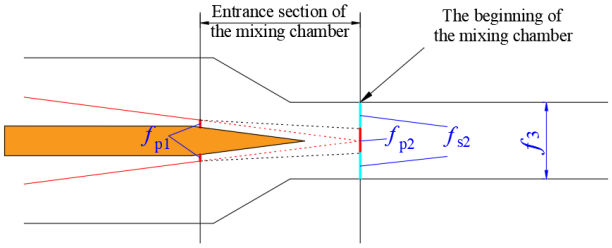

Fig. 4 Simplified mixing chamber entrance section and mixing chamber

When the nozzle is completely blocked by the needle, the position of the needle tip in the mixing chamber is regarded as the starting position of the mixing chamber. It is considered that the primary flow at this position is a completely solid cylindrical jet, and the part of the chamber before this position is divided into the entrance section of the mixing chamber (characterized by the velocity coefficient φ_5). The simplified characteristic equation is:

$$h = \frac{2\varphi_1^2\varphi_4\varphi_5}{m} + 2\varphi_1^2\varphi_4\varphi_5\frac{u^2}{m(\varphi_5 m - 1)} - \frac{\varphi_1^2\varphi_5^2}{\varphi_2^2}\frac{u^2}{(\varphi_5 m - 1)^2} - \varphi_1^2(2-\varphi_3^2)\frac{(1+u)^2}{m^2} \tag{18}$$

It can be seen from equation (17) and (18) that when the values of φ_1-φ_5 are given, the characteristics of the jet pump are determined by the flow ratio *u* and

the area ratio m. In most application scenarios, the user does not care about the internal flow of the jet pump, but only pays attention to the overall operating parameters of the jet pump. Equation (1), (4), (17) and (18) can be used to estimate the flow and pressure of a specific jet pump under given operating conditions, providing data support for designing jet pumps or analyzing systems containing jet pumps.

At present, the values of $\varphi_1 - \varphi_4$ are mostly the following empirical values. $\varphi_1 = 0.95$, $\varphi_2 = 0.925$, $\varphi_3 = 0.9$, $\varphi_4 = 0.975$. In fact, the values of them are related to the structure, internal wall surface roughness and the flow state in the jet pump. The velocity of the flow at the nozzle outlet, the inlet and the outlet of the mixing chamber is relatively large, and the flow pattern is basically the same, so the influence of the flow state on the velocity coefficient is not considered. The difference in the structure of AJP and FJP will inevitably cause the deviation of the velocity coefficients. Moreover, the influence of the needle on the flow in the jet pump is not only in the nozzle, but also in the suction chamber and the mixing chamber. It is not enough to modify the velocity coefficient of the nozzle. Therefore, all coefficients need to be corrected so that the mathematical model can be accurately used in the calculation about AJP.

3. EXPERIMENT

3.1 Experiment device

The structure of the tested AJP is shown in *Fig. 5*. The needle is added to adjust the nozzle outlet area by changing its position. In order to facilitate the installation of the needle, the inlet position of the primary flow is adjusted. The primary flow enters the cavity through the inlet, and then is ejected through the nozzle, which has an entrainment effect on the secondary flow in the suction chamber. The velocity direction of the primary flow at the inlet is at an angle of 90° with the velocity direction at the nozzle, which is different from the jet pump mentioned above. The main structural parameters of the adjustable pump in *Fig. 5* include the following: the diameter of the inlet of the primary flow D_p, the diameter of the suction duct D_s, the diameter of the diffuser outlet D_c, the length of the nozzle L_0, the length from the nozzle outlet to the throat L_c, the length of the throat L_h, the diameter of the nozzle outlet d_1, the diameter of the throat d_3, the inclined angle of the throat α_1 and α_2, the inclined angle of the diffuser β. The above structural parameters are designed as shown in *Table 1*.

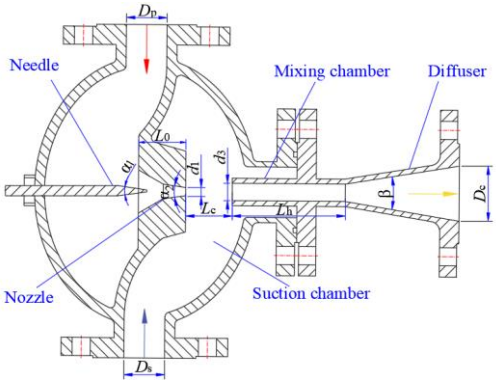

Fig. 5 The structure of the tested adjustable jet pump

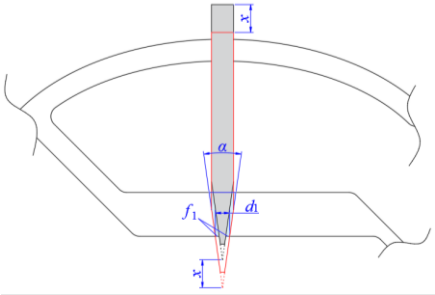

Fig. 6. The relationship between the position of the nozzle and the nozzle outlet area

For the purpose of studying the performance of the jet pump under different area ratios, the position of the needle was altered to change the area of the nozzle outlet. As shown in *Fig. 6*, the stroke of the starting position (indicated by the red line) is 0, where the needle completely blocks the nozzle. When the stroke (indicated by the gray shading) is x, the nozzle outlet area f_1 is determined by *eq*. 19.

$$f_1 = \pi\left(\frac{d_1^2}{4} - \left(\frac{d_1}{2tan\frac{\alpha_2}{2}} - x\right)^2\right) \tag{19}$$

An experiment is carried out on the adjustable jet pump with the needle in 6 different positions in this research. The specific stroke, nozzle outlet area and area ratio are shown in *Table 2*. The relative position of the spray needle and the mixing chamber is shown in *Fig. 7*. It can be seen that when the stroke of the needle x<15, the top will be in the mixing chamber.

Table 1 The parameters of the tested adjustable jet pump

Parameters	D_p	D_s	D_c	d_1	d_3	L_0	L_c	L_h	α_1	α_2	β
Values	37mm	37mm	50mm	9mm	11mm	20mm	10.2mm	85mm	60°	16°	16°

Table 2 The stroke and nozzle outlet area and area ratio selected in the experiment

Stroke x (mm)	4.5	6	9	12	15	18
Area of nozzle outlet f_{p1} (mm^2)	16.63	21.61	30.74	38.75	45.64	51.42
Area ratio m	5.716	4.397	3.092	2.453	2.082	1.848

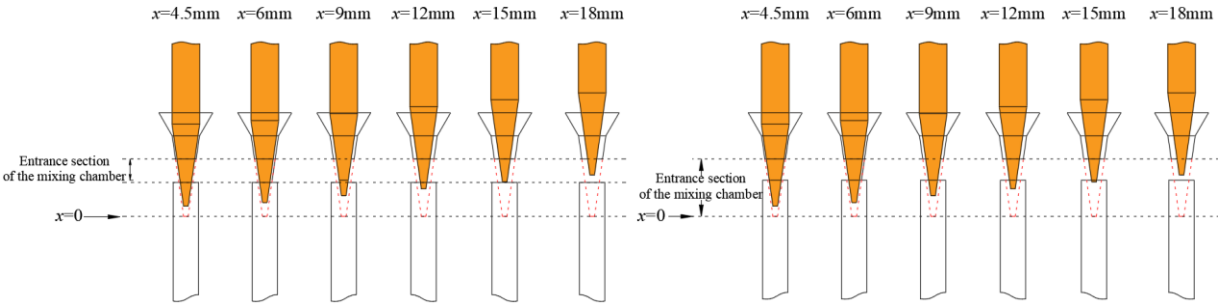

Fig. 7 The relative position of the needle and the mixing chamber (left: original; right: simplified)

3.2 Test rig and scheme

As illustrated in *Fig. 8*, the test rig used in this research is designed according to the application scenario of the jet pump acting as a water mixing device in heating system. The high-pressure supply water (*primary fow*) pumped by the circulating water pump passes through the jet pump to entrain part of the low-pressure return water (*secondary flow*) from the user, and the two flows are mixed and supplied to the user. The remaining part of the return water is pressurized by the water pump to continue to flow into the jet pump, forming a closed loop system. The main function of the water tank (1 in *Fig. 8*) is to stabilize the pressure of the return water and. The user in the system is replaced with a ball valve (11 in *Fig. 8*) to simulate its hydraulic resistance.

During the experiment, the liquid level of the water tank remains unchanged to ensure that the inlet pressure of the secondary flow P_s is always within a small range. The inlet pressure and flow rate of the primary flow P_p, G_p are adjusted by changing the operating frequency of the circulating water pump. The flow rate of the secondary flow G_s and the outlet pressure of the mixed flow P_c are controlled by the resistance of the user (the opening of the ball valve). Pressure gauges (8,9,10 in *Fig. 8*) are installed at the inlet of the primary flow and the secondary flow and the outlet of the mixed flow to monitor the inlet and outlet pressures of the three flows. The accuracy of all pressure gauges is 0.1%. The flow rates are measured with turbine flow meters (5,6,7 in *Fig. 8*), and the accuracy of all flow meters is 0.5%. The clean water used in the experiment is at room temperature and replaced in time, so the density change caused by the variation of temperature is negligible during the experiment.

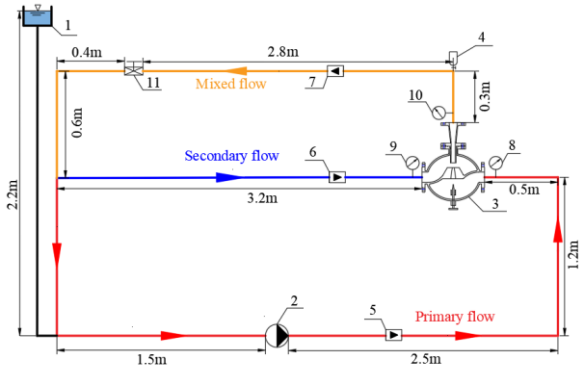

1. Tank 2. Variable frequency water pump 3. Adjustable pump 4. Vent 5,6,7. Flow meter 8,9,10. Pressure gauge 11. Ball valve

Fig. 8 Sketch of the experimental rig

In order to solve velocity coefficient of the nozzle φ_1, firstly, by adjusting the frequency of the water pump to change the working pressure difference. The primary flow rate is recorded under different working pressure differences when the jet pump is at the same area ratio (the opening of valve (11 in *Fig. 8*) remains unchanged during the experiment). Then three different working pressure differences are selected, and the flow rate of the secondary flow is changed by adjusting the opening of the valve (11 in *Fig. 8*) to obtain the performance curve of the jet pump under the area ratio. Follow the above method to test the jet pump when the needle is in different strokes.

3.3 Solving method of velocity coefficients

According to equation (20), the velocity coefficients under different working pressure differences are obtained, and the average value is taken as the final velocity coefficient of the nozzle under the corresponding area ratio.

$$\varphi_1 = \frac{G_p}{f_{p1}\sqrt{2\rho_{p1}\Delta P_p}} \tag{20}$$

After the nozzle velocity coefficient is obtained, the coefficients $\varphi_2 - \varphi_5$ are obtained by fitting the experimental data. In this research, genetic algorithm is

used to transform the problem of solving coefficients into the problem of optimal solution of the objective function. The objective function is to find the minimum value of the residual sum of squares of the predicted value and the true value, namely

$$min[\sum_{i=1}^{n}(h - h_{pre})^2]$$

The coefficients φ_3 and φ_4 are basically connected to the empirical value. The coefficient φ_2 will be very different from that of FJP. On the one hand, the structure of the suction chamber of the AJP tested in the experiment is very different from that of the fixed type. On the other hand, in the inlet section of the mixing chamber, the presence of the needle will affect the flow of the secondary flow. the value range of each coefficient during optimization is as follows:

lb = [0.60, 0.88, 0.955, 0.8], *ub* = [1.5, 0.92, 0.995, 1.00].

The obtained velocity coefficients of the mixing chamber and the diffuser φ_3 and φ_4 are averaged as the final velocity coefficient values. The function relationship between coefficients φ_1, φ_2, φ_5 and area ratio *m* is obtained by nonlinear fitting.

4. RESULT AND DISCUSSION

In this study, in view of the original and simplified situation, the coefficients φ_1-φ_5 were solved when the stroke of the needle *x* is 4.5, 6, 9, 12, 18mm (the corresponding area ratio *m*=5.716, 4.398, 3.092, 2.453, 1.848), respectively. The coefficients obtained by the optimization are substituted into the original and simplified characteristic equations respectively, and the predicted values obtained from the equations (17) and (18) are compared with the experimental results.

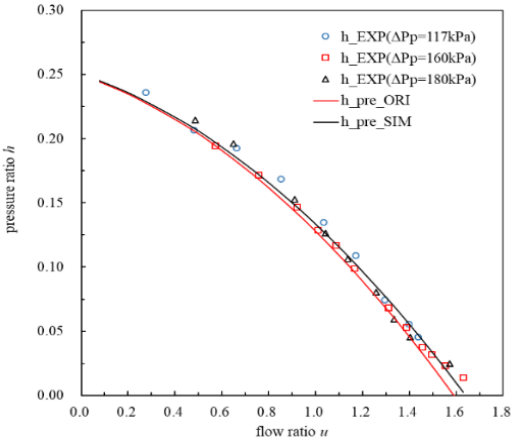

Fig. 9 x=4.5mm, m=5.716

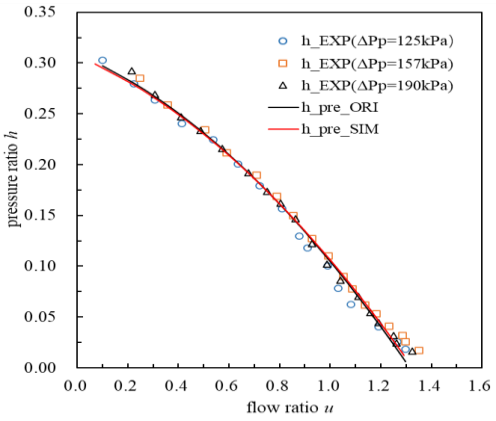

Fig. 10 x=6mm, m=4.398

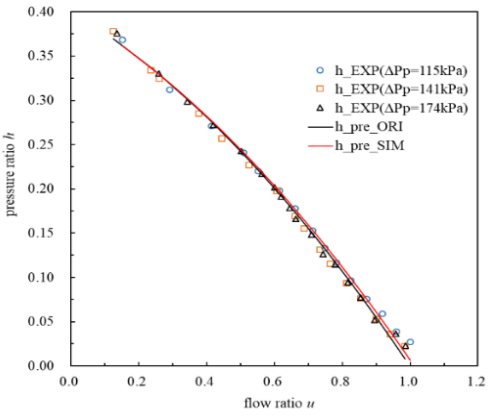

Fig. 11 x=9mm, m=3.092

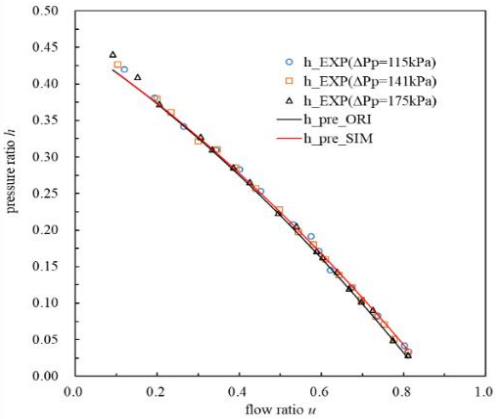

Fig. 12 x=12mm, m=4.453

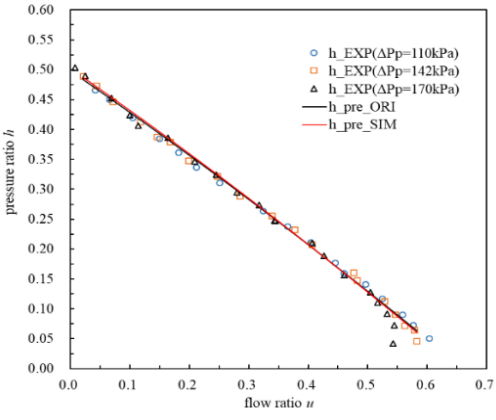

Fig. 13 x=18mm, m=1.848

Fig. 9- Fig. 13 show that the theoretical curve is very close to the experimental results. In order to further estimate the accuracy of the solved coefficients, the correlation coefficient R^2 is introduced. The closer the value of R^2 is to 1, the higher the degree of closeness between the predicted value and the true value. R^2 is defined as follows:

$$R^2 = 1 - \frac{\sum_{i=1}^{n}\left(h - h_{\mathrm{pre}}\right)^2}{\sum_{i=1}^{n}\left(h - \bar{h}\right)^2}$$

The obtained coefficients φ_1-φ_5 are shown in *Table 3*. The minimum R^2 is 0.981, which can meet engineering requirement.

Table 3 The values of velocity coefficients φ_1-φ_4 and jet cross-sectional area ratio φ_5

x/mm	m	Scheme	ϕ1	ϕ2	ϕ3	ϕ4	ϕ5	R^2
4.5	5.716	Original	0.914	0.778	0.890	0.959	1.000	0.981
		Simplified		0.666	0.899	0.960	1.000	0.984
6	4.398	Original	0.930	0.815	0.900	0.960	0.958	0.990
		Simplified		0.710	0.897	0.965	0.949	0.995
9	3.092	Original	0.960	0.919	0.900	0.965	0.898	0.995
		Simplified		0.832	0.902	0.968	0.896	0.995
12	2.453	Original	0.971	1.048	0.904	0.967	0.866	0.996
		Simplified		0.997	0.900	0.965	0.865	0.997
18	1.848	Original	0.994	1.357	0.903	0.964	0.816	0.995
		Simplified		1.329	0.900	0.965	0.820	0.995

Fig. 14 shows the changing trend of coefficients φ_1 - φ_5 with increasing needle stroke. It can be seen from the figure that both in original scene and the simplified one, the velocity coefficients of the mixing chamber and the diffuser φ_3 and φ_4 are independent of the presence of the needle. This is due to the fact that the structure of the diffuser and the mixing chamber hardly changed with the movement of the needle. The average values of the velocity coefficients of the diffuser in the two scenarios φ_{3_ORI} and φ_{3_SIM} are 0.8893 and 0.8994, respectively, and that of the mixing chamber φ_{4_ORI} and φ_{4_SIM} are 0.9630 and 0.9648, respectively. The simplified mixing chamber velocity coefficient is slightly larger than the original, which is due to the slight difference caused by the needle.

When the exit area of the nozzle expands with the increase of the needle stroke, the local resistance at the nozzle decreases and the velocity coefficient of the nozzle $\varphi_1$becomes larger. It should be noted that as the nozzle opening increases, the coefficient φ_1 may be greater than 1. This is because the nozzle outlet pressure of the primary flow P_{p1} will be lower than the secondary flow inlet pressure P_s, and the calculated φ_1 may be greater than 1. The velocity coefficient of the inlet section of the mixing chamber φ_2 changes greatly with the increase of the needle stroke *x*. When the stroke of the needle *x* is relatively small, the volume of the needle in the inlet section of the mixing chamber is larger, which greatly hinders the secondary flow from entering the mixing chamber, so the velocity coefficient φ_2 is small. As the stroke of the needle increases, the hindrance decreases rapidly. At the same time, the increase of the nozzle area makes the more primary flow sprayed, which will locally mix with the secondary flow before reaching the mixing chamber and exchange energy. Therefore, a situation where φ_2 is greater than 1 will occur. Under the same needle position, φ_2 in the original scenario is larger than the simplified one. This is because the simplified mixing chamber entrance section contains a part of the mixing chamber. And the smaller the stroke of the needle, the larger the volume of the needle in this part, which leads to the greater the difference in φ_2 between the two scenarios. As the area ratio *m* decreases, the larger the jet cross-section of the primary flow is, the faster the boundary layer expands, and the greater the jet cross-section changes when it reaches the inlet cross-section of the mixing chamber. Therefore, φ_5 gradually decreases as the stroke increases.

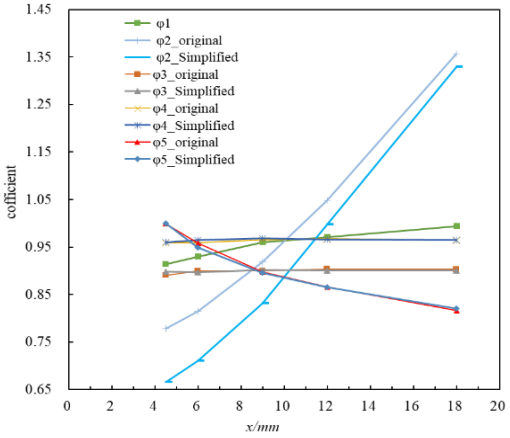

Fig. 14 Change trend of coefficients with area ratio m

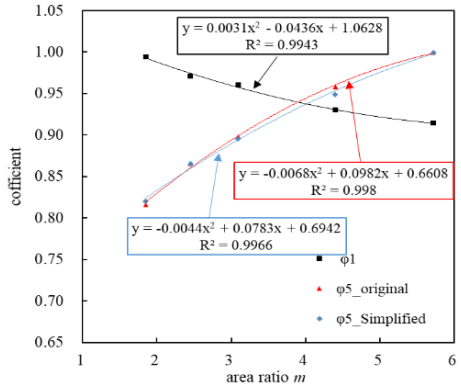

Fig. 15 the relationship between φ_1, φ_5 and m

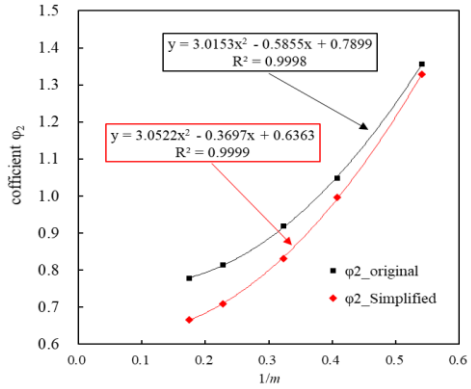

Fig. 16 The relationship between φ_2, and 1/m

The functional relationship between the coefficients and the area ratio is shown in *Fig. 15* and *Fig. 16*. The coefficients φ_1 and φ_5 have a good quadratic function relationship with area ratio *m* respectively. There is also a good quadratic relationship between the coefficient φ_2 and the reciprocal of the area ratio (1/*m*). The fitted function relationship between the coefficients and the area ratio was used to solve the coefficient value when x=15mm (m=2.082), and the characteristic equation was used to predict the pressure ratio *h*. At the same time, when the inlet and outlet pressures are known, the flow rate of the primary flow and the mixed flow is calculated through the mathematical model.

Fig. 17 shows the comparison of predicted value with real value. The average error of the primary flow is 2.04%, and the average error of the mixed flow obtained from the original equation and the simplified equation are 1.23% and 1.26%, respectively. The maximum error of the primary flow is 4.82%, and the maximum error of the mixed flow obtained from the original equation and the simplified equation are 2.76% and 3.09%, respectively. The R^2 of the primary flow rate is 0.978. The R^2 of pressure ratio obtained from the two equations are 0.992 and 0.996, respectively; the R^2 of the mixed flow is 0.992 and 0.991, respectively. The resulting characteristic equation of AJP can be used for calculations related to the type of adjustable jet pump.

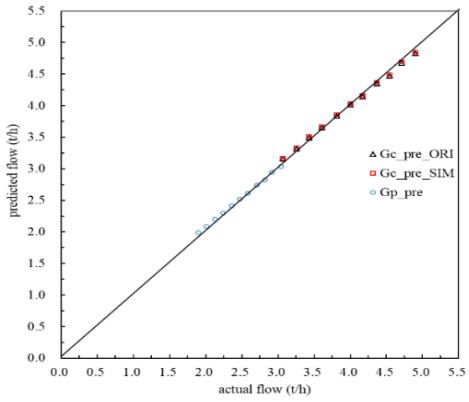

(a)

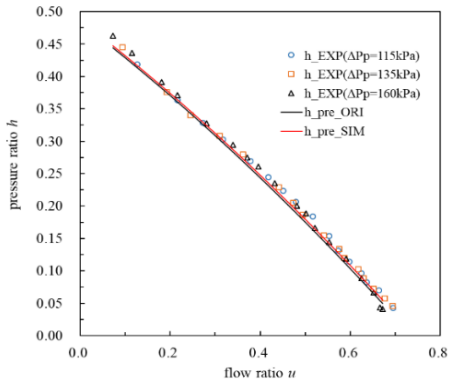

(b)

Fig. 17 Error analysis（x=15mm, m=2.082）
(a) pressure ratio (b)flow rate

5. CONCLUSIONS

In this study, the coefficients of the AJP were identified based on the experimental data by using the genetic algorithm optimization method. First, based on the existing mathematical equations of jet pumps, the position of the needle and the cross-sectional expansion of the primary flow jet are considered. Introducing the jet cross-sectional area ratio, the characteristic equation of AJP was improved and simplified. Then, based on the experimental data, the genetic optimization algorithm is

used to identify the coefficients of the tested AJP under different area ratios. Then the function relations between each coefficient value obtained by optimization and the area ratio was fitted. Finally, the accuracy of the coefficients and function relations obtained by the solution is verified.

According to the results of above, the following conclusions can be presented:

(1) When the area ratio is relatively small, the expansion of the jet cross-section of the primary flow between the nozzle outlet and the inlet of the mixing chamber should be considered during establishing mathematic equations of AJP.

(2) The presence of the needle has a negligible effect on the velocity coefficients of the diffuser and the mixing chamber φ_3 and φ_4. Both φ_3 and φ_4 are relatively close to the experience value.

(3) Both the velocity coefficient of the nozzle φ_1 and the jet cross-sectional area ratio φ_5 have a quadratic function relationship with the area ratio *m*; the velocity coefficient of the inlet section of the mixing chamber φ_2 has a quadratic function relationship with the reciprocal of the area ratio *m*.

(4) After verification, the average error of the flow rate predicted by the original equation and the simplified equation is less than 2%. This method of solving the velocity coefficient of the jet pump is reliable.

ACKNOWLEDGEMENT

This work was financially supported by National Key R&D Program of China (2021YFE0116200).

REFERENCE

[1]Aldaş, K., & Yapıcı, R. (2014). Investigation of Effects of Scale and Surface Roughness on Efficiency of Water Jet Pumps Using CFD. *Engineering Applications of Computational Fluid Mechanics, 8*(1), 14-25.

[2]Beithou, N., & Aybar, H. S. (2000). A mathematical model for steam-driven jet pump. *International Journal of Multiphase Flow, 26*(10), 1609-1619.

[3]Li, Y., Wang, W., Yao, S., Wei, W., Xiao, Q., & Li, S. (2019). Numerical Study on Effect of Ocean Conditions on Jet Pump Cavitation Characteristics for Marine Nuclear Power Plants. *Nuclear Power Engineering, 40*(5), 135-139.

[4]Liu, F., Li, D., & Zeng, X. (2017, 2017Oct 19-22). *Research on Energy Saving Technology of Distributing Combined Adjustable Jet Pump.* Paper presented at the 10th International Symposium on Heating, Ventilation and Air Conditioning (ISHVAC), Jinan, PEOPLES R CHINA.

[5]Liu, X. L., Zhan, Q. Q., & Lia, Y. A. (2017, Oct 19-22). *The application analysis of jet pump in heating system.* Paper presented at the 10th International Symposium on Heating, Ventilation and Air Conditioning (ISHVAC), Jinan, PEOPLES R CHINA.

[6]Long, X., Xu, M., Lyu, Q., & Zou, J. (2016). Impact of the internal flow in a jet fish pump on the fish. *Ocean Engineering, 126*, 313-320.

[7]Long, X., Zhang, J., Wang, Q., Xiao, L., Xu, M., Lyu, Q., & Ji, B. (2016). Experimental investigation on the performance of jet pump cavitation reactor at different area ratios. *Experimental Thermal and Fluid Science, 78*, 309-321.

[8]Lu, H., & Lu, D. (2011). Strive to Explore the Scientific and Technological Knowledge, Broaden the Injection Technology Development. *Frontier Science, 5*(3), 32-39.

[9]Lu, Y., Liu, H., Wang, X., & Wang, H. (2021). Study of the Operating Characteristics for the High-Speed Water Jet Pump Installed on the Underwater Vehicle with Different Cruising Speeds. *Journal of Marine Science and Engineering, 9*(3).

[10]Neto, I. E. L. (2011). Maximum suction lift of water jet pumps. *Journal of Mechanical Science and Technology, 25*(2), 391-394. doi:10.1007/s12206-010-1221-7

[11]Reis, L. B., & Gioria, R. D. (2021). Optimization of liquid jet ejector geometry and its impact on flow fields. *Applied Thermal Engineering, 194*.

[12]Sheha, A. A. A., Nasr, M., Hosien, M. A., & Wahba, E. M. (2018). Computational and Experimental Study on the Water-Jet Pump Performance. *Journal of Applied Fluid Mechanics, 11*(4), 1013-1020.

[13]Wang, H., & Wang, H. (2019). Enhance Hydraulic balance of a District Cooling System with Multiple Jet Pump. In J. Yan, H. X. Yang, H. Li, & X. Chen (Eds.), *Innovative Solutions for Energy Transitions* (Vol. 158, pp. 2536-2542).

[14]Winoto, S. H., Li, H., & Shah, D. A. (2000). Efficiency of jet pumps. *Journal of Hydraulic Engineering-Asce, 126*(2), 150-156.

[15]Zhang, Y., Xiong, N., Ge, Z., Zhang, Y., Hao, J., & Yang, Z. (2020). A novel cascade heating system for waste heat recovery in the combined heat and power plant integrating with the steam jet pump. *Applied Energy, 278*.

[16]Zhu, J. M., Long, X. P., Zhang, S. B., & Lu, X. (2012). Experiment on performance of adjustable jet pump. *IOP Conference Series: Earth and Environmental Science, 15*(6).